JOURNAL OF MATERIALS SCIENCE 32 (1997) 4237–4245

Morphology of the poly(vinyl alcohol)–poly(vinyl acetate) copolymer in macrodefect-free composites: a ^{13}C magic-angle-spinning nuclear magnetic resonance and ^{1}H spin-diffusion study

ANGIOLINA COMOTTI*‡, ROBERTO SIMONUTTI, PIERO SOZZANI
Dipartimento di Scienza dei Materiali, Università di Milano, via Emanueli 15, 20126-Milano, Italy

A study was made of the macrodefect-free (MDF) composite based on aluminate cement and a poly(vinyl alcohol)–poly(vinyl acetate) (PVAc) copolymer by ^{13}C cross-polarization magic-angle-spinning nuclear magnetic resonance. The spectra were run on both the copolymer and the MDF composite in order to observe the atomic environments of the carbon nuclei. An analysis of the intramolecular hydrogen bonds showed a stronger modification in the sample containing $CaAl_2O_4$ (CA) than in that containing $Ca_3Al_2O_6$ (C_3A). From the spectra, it was seen that deacetylation had occurred, and that there was interaction between acetate groups and the calcium and aluminium ions. Proton relaxation times both in the laboratory frame, T_1(H), and in the rotating frame, $T_{1\rho}$(H), were exploited for the study of the dimension of the polymer matrix in MDF composites. An extended interphase was identified in the composite containing CA. A comparison with the behaviour of the composite based on silicates Ca_3SiO_5–PVAc highlights the better mixing of the phases in the MDF composites containing CA.

1. Introduction

The term macrodefect free (MDF) is applied to cement-based composites with good mechanical properties [1, 2], i.e., high flexural strength and high Young's modulus. Such composites represent a new class of materials, made by combining water with a hydraulic cement and a water-soluble polymer, and subjecting the product to high shear mixing and a curing–drying process [3–5]. The most well-known composites are made of calcium aluminates ($CaAl_2O_4$ (CA) and $CaAl_4O_7$ (CA_2)) and a poly(vinyl alcohol)–poly(vinyl acetate) (PVAc) copolymer.

The composite is characterized by high strength and toughness because the polymer affects the rheology of the mixture; in addition the high-pressure procedure helps to reduce material porosity. Also the interphase between the organic and inorganic matrices, formed by chemical bonding and physical interaction, imparts improved mechanical properties. An amorphous layer at the ceramic–polymer interface has been observed [6–10] and has been found to consist of a metastable hydrated aluminate product and a polymer matrix cross-linked with the aluminium atoms. Furthermore, the role of the interphase has been observed during both wet and dry mechanical tests; at the nanometre level, the microstructure and composition of this interphase has mainly been studied by electron microscopy (transmission electron microscopy, scanning electron microscopy and high-resolution electron microscopy) and by X-ray photoelectron spectroscopy.

MDF materials have also been characterized by other methods [11–15], including solution chemistry, X-ray diffraction (XRD), infrared and conduction calorimetry. Groves and co-workers [11–13] studied the hydration of calcium aluminate in the presence of the PVAc copolymer and proposed the formation of a cross-linked polymer phase with aluminate ions. Infrared measurements indicate the presence of a metal carboxylate product and XRD data suggest the formation of hemihydrate calcium acetate. Edmonds and co-workers [14, 15] focused on the hydration of aluminate cements with PVAc copolymers at different acetate group percentages. They confirmed the interaction of the aluminium ions with the polymer and suggested the formation of either acetate ions or an ester group complexed to a metal ion. Moreover, they observed that, in the early stages of the hydration, metal ions interact with the ester groups.

* Author to whom all correspondence should be addressed.
‡ Formerly at Italcemente group, Bergamo.

Solid-state magic-angle-spinning (MAS) nuclear magnetic resonance (NMR) is a technique highly sensitive to the local environment of the observed nuclei and, by the selection of proper pulse sequences, it can give a measurement of domains at the nanometer level. A MAS NMR study on MDF materials based on Ca_3SiO_5 (C_3S) had already been performed by the present authors, observing ^{13}C and ^{29}Si nuclei and exploiting the proton spin diffusion phenomenon across the heterogeneous interfaces for the detection of the adhesion between the phases [16]. Furthermore, the hydration of calcium aluminate powders has been studied by both ^{27}Al MAS NMR [17–21] and wide-line proton relaxation times [22]. On the other hand, MDF composites based on aluminates have rarely been characterized by solid-state NMR techniques [23, 24]. Owing to the low concentration of water (water-to-cement ratio, 0.1) and the kinetics of the reaction in MDF composites, the formation of an extensive inorganic hydrated phase is precluded and, therefore, the detection by ^{27}Al MAS NMR of the hydrated inorganic phase may be difficult. Thus the study of the composite materials was made by combining ^{1}H and ^{13}C cross-polarization (CP) MAS NMR spectroscopy.

The composite materials that we studied were obtained by mixing, under a high-pressure procedure, one of the most reactive components of aluminate cements, CA, and the PVAc copolymer. A comparative study of a material containing a less reactive inorganic compound, C_3A, was performed. The reaction products (acetates) and the physical interactions, such as hydrogen bonding, were characterized. The dimension of the polymer phase and of the interphase in the composite were determined by measuring the proton relaxation times in both the laboratory and the rotating frame, calculated by transferring the magnetization to ^{13}C nuclei. The proton relaxation of the polymer materials was found to depend essentially on the molecular motions, but it is also affected by the phenomenon of spin diffusion [25] which gives spatial information. In our MDF materials the proton relaxation times, selectively detected by ^{13}C, are influenced by the propagation of the magnetization from the organic to the inorganic phase and by the intimacy of the phases.

2. Experimental procedure

2.1. Materials

An 80% hydrolysed PVAc was purchased from Nippon Synthetic Chemical Industry Co. Ltd, Japan (Gohsenol KH-17s) with a degree of polymerization of 300–3000 and a viscosity (4% in water; 20 °C) of 32–38 mPa s. The microstructure of PVAc in solution was determined by ^{13}C and ^{1}H NMR [26–29].

The synthesis of C_3A and CA was carried out using stoichiometric quantities of calcium carbonate and Al_2O_3. The relative mixtures were repeatedly ground and heated, C_3A at 1400 °C and CA at 1300 °C, until equilibrium conditions were reached. The powders obtained were characterized by XRD and optical microscopy.

Each powder was then mixed with an 80% hydrolysed PVAc copolymer and distilled water and then pressed at 80 bar and heated at 353 K for 10 min in air (pressed samples). The composition of the pressed samples was as follows: sample PVAc–C_3A, 10 g of C_3A with 1 g of PVAc; sample PVAc–CA, 10 g of CA with 1 g of PVAc; both of these underwent the above-mentioned processing with a water-to-cement ratio of 0.1. Some of these samples were subjected to further curing at 353 K for 24 h in air (cured samples) [3]. Both the flat sheets of the composite (pressed samples) and the cured samples were analysed by MAS NMR. XRD profiles of the powders were obtained with a Siemens D5000 diffractometer, using Cu$K\alpha$ radiation and a diffracted-beam monochromator.

2.2. Nuclear magnetic resonance spectroscopy

High-resolution ^{13}C MAS NMR spectra were obtained at 75.5 MHz on a CXP300 Bruker instrument operating at a static magnetic field of 7.4 T. A MAS Bruker probe was used with 7 mm ZrO_2 rotors spinning at a standard speed of 5 kHz. CP spectra were determined at 1 ms contact time. A high-power proton decoupling (DD) field of 15 G was applied, the delay between pulses being 5 s for CP MAS. Spin temperature alternation was applied [30]. For each spectrum about 5000–10 000 transients were collected. A 90° pulse for proton of 3.5 μs was used. The resolution for carbon was checked on glycine (width at half-height, 26 Hz). Crystalline polyethylene was taken as an external reference at 33.63 ppm for tetramethylsilane. Relaxation measurements of T_1 (^{13}C) were performed by the Torchia [31] method.

2.3. Pulse sequence description and space-domain determination

The pulse sequence applied to measure spin diffusion among protons in the high-resolution mode are shown in Fig. 1. Proton relaxation times $T_{1\rho}(H)$ in the rotating frame were measured indirectly by varying the length of a ^{1}H spin-lock period prior to a fixed proton–carbon CP contact period (Fig. 1a). Proton relaxation times, $T_1(H)$, in the laboratory frame were measured by applying an inversion–recovery sequence to the ^{1}H and successively transferring the proton magnetization to the rare nuclei by the CP contact period (Fig. 1b). The relaxation rates were determined using a non-linear least-squares best-fit procedure of the intensities, $M(\tau)$, in the carbon domain, using one exponential function or the sum of two:

$$M(\tau) = \sum_i M_{0i} \exp\left(-\frac{\tau}{T_{1i}}\right) \quad (1)$$

An array of experiments with variable CP contact times [32] allowed us to measure the relaxation times, T_{CH} and $T_{1\rho}(H)$, from the fitting of $M(\tau)$ (Fig. 1c):

$$M(\tau) = M_0 \frac{\exp[-\tau/T_{1\rho}(H)] - \exp(-\tau/T_{CH})}{1 - T_{CH}/T_{1\rho}(H)} \quad (2)$$

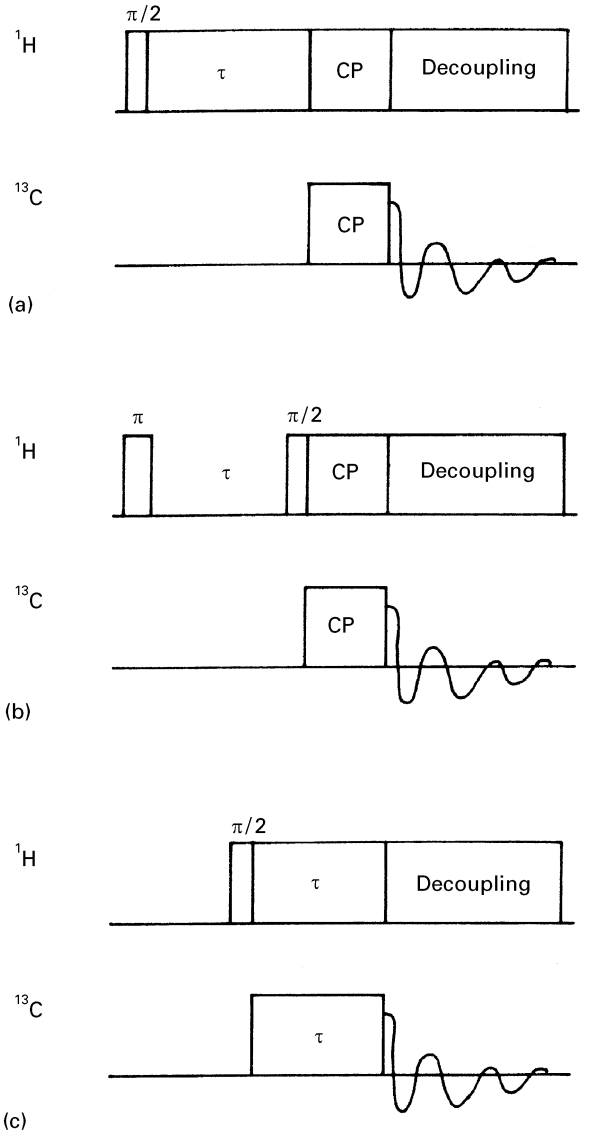

Figure 1 Pulse sequences applied to obtain high-resolution spectra and the measurement of abundant nuclei relaxation times. Pulse sequence applied for the measurement of the relaxation times (a) in the rotating frame, $T_{1\rho}$(H) and (b) in the laboratory frame, T_1(H). (c) CP pulse sequence.

Equation 2 consists of two terms: one describes the build-up of ^{13}C magnetization with the time constant T_{CH} and the other is dominated by the relaxation in the rotating frame, $T_{1\rho}$(H). Equation 2 is valid when $T_{1\rho}(^{13}C)$ is much slower than $T_{1\rho}$(H).

It is the fluctuation of the dipolar coupling generated by the motion of the molecules that causes the proton relaxation [25, 33]. The frequency range of such fluctuations determines the values of the proton relaxation times, both in the laboratory frame, T_1(H), and in the rotating frame, $T_{1\rho}$(H). The T_1(H) values are of the order of seconds, and those of $T_{1\rho}$(H) of the order of milliseconds.

In solids, for strongly homonuclear coupled nuclei, nuclear magnetization can migrate among the regions through a flip–flop mechanism. The magnetization path length is dominated by the diffusion phenomenon. Proton relaxation times are therefore subjected to the spin-diffusion effect which, depending on the size of the regions, averages out the proton relaxation values [34–42]. If the region domains are large with respect to the time necessary for the relaxation, then the time constant measured is the intrinsic relaxation of the phase but, if the size of the regions is smaller than the space travelled by the magnetization diffusion, the proton relaxation times may be lowered or raised as a function of the next region proton relaxation time. It can be concluded that $T_{1\rho}$(H) and T_1(H) relaxation times give an insight into phase heterogeneities of different dimensions, from a few nanometres to tenths of a nanometre.

In polymer materials the abundant proton density allows efficient spin diffusion. Many papers have been published on the morphology of crystalline and amorphous regions in homopolymers based on this technique [37, 42, 43] and on the polymer blend homogeneity at the nanometre level [38–41, 44]; several models [34, 37, 45] have been proposed to calculate the spatial domains from T_1(H) and $T_{1\rho}$(H). In an isotropic regime of propagation of magnetization and considering a three-dimensional model the average mean square distance, $\langle L^2 \rangle$, can be determined as follows:

$$\langle L^2 \rangle = 6D\tau \tag{3}$$

where D is the spin-diffusion coefficient and τ represents T_1(H) or $T_{1\rho}$(H). The diffusion coefficient measured by Douglass and Jones [46] for *n*-alkanes is 6.2×10^{-16} m^2 s^{-1} in the laboratory frame and is proportional to the proton concentration to the power 1/3. We can assume that in our polymer system the diffusion coefficient corresponds to that of *n*-alkanes, the proton density being almost coincident. In the presence of a spin-lock field along the x axis, D was calculated to be half of that in the absence of the spin-lock field, since spin diffusion is proportional to $(3 \cos \theta^2 - 1)$ [37]. Thus T_1(H) values, which show longer relaxation times and a faster diffusion coefficient, are sensitive to larger dimensional scales than $T_{1\rho}$(H).

If no such diffusion coefficient is available, a rough estimation of the mean square displacement is obtained from [33]

$$\langle L^2 \rangle \approx \frac{\langle l_0^2 \rangle}{T_2 \tau} \tag{4}$$

where l_0 is the distance between protons (about 0.1 nm) and T_2 is the spin–spin relaxation ($T_2 \approx 10$ μs). In fact, the reciprocal of T_2 corresponds to the transition rate of the flip–flop phenomenon. For the acetate phases the last equation will be considered.

3. Results and discussion

PVAc copolymer, obtained using 80% deacetylated poly(vinyl acetate), was adopted as the starting polymer. Under the basic conditions used in the preparation of the composite the PVAc could further deacetylate, forming poly(vinyl alcohol), acetate groups (Fig. 2) and a polymer–ceramic interphase [6–10]. This process of deacetylation can occur either partially or completely.

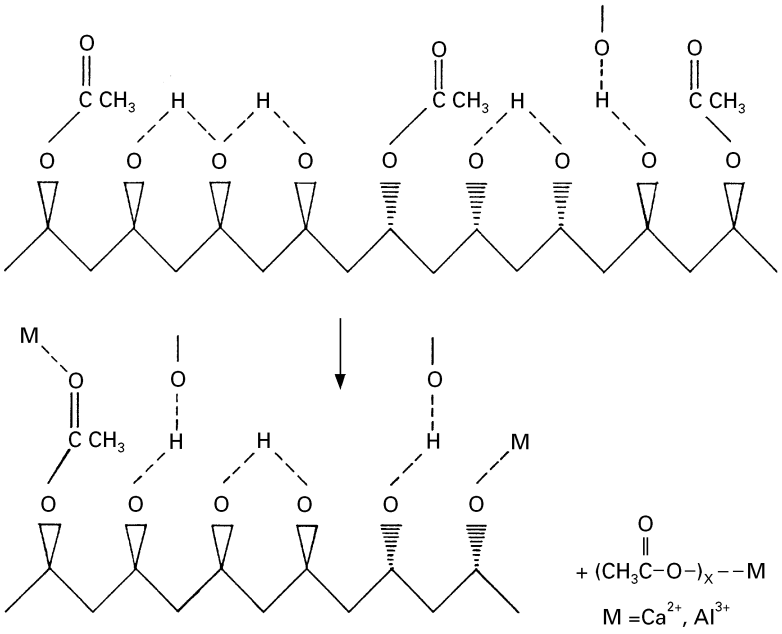

Figure 2 Schematic representation of PVAc copolymer and the organic products formed during the process to form MDF composites.

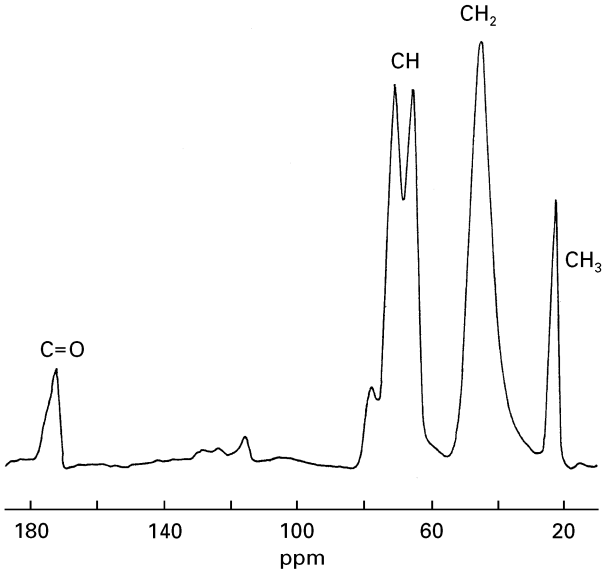

Figure 3 75.5 MHz ^{13}C CP MAS NMR spectra of PVAc. The CP mixing time was 1 ms. No window functions were applied.

TABLE I $T_1(^{13}C)$ carbon relaxation times of PVAc, as derived from the CP T_1 sequence (Torchia's sequence; see text), where a biexponential best-fitting minimum square was applied and the values are affected by a 10% error

Assignment	Chemical shift (ppm)	$T_1(^{13}C)$ (s)	$T_1(^{13}C)$ (relative percentage)
CH_3	22.5	16.3 ± 0.6	
CH_2	45.4	$11.1 \pm 1.5/94.2 \pm 11.4$	48/52
CH	65.7	$12.8 \pm 1.6/86.7 \pm 7.9$	42/58
CH	71.2	$11.6 \pm 2.1/83.6 \pm 8.2$	35/65
CH	77.4	$2.3 \pm 1.1/58.3 \pm 4.3$	16/84
CO	171.8	69.5 ± 1.1	

3.1. Characterization of poly(vinyl alcohol)–poly(vinyl acetate)

Fig. 3 shows the ^{13}C MAS NMR spectrum of PVAc. It should be emphasized that the ^{13}C MAS NMR spectrum is especially informative about hydrogen bonding, the most striking effect being the presence of three peaks for the methine atoms [47]. In this kind of polymer the chemical shift of the methine carbons depends on the number of intramolecular hydrogen bonds; this number is mainly influenced by the stereochemistry of the polymer: mm triads may give rise to two intramolecular hydrogen bonds and mr to one.

$T_1(^{13}C)$ relaxation time measurements showed two exponential decays of about 80 s and 10 s for most signals (Table I) and were assigned to the crystalline and amorphous phases respectively [47–49]. The $T_1(^{13}C)$ are confirmed by the work of Terao *et al.* [47].

^{1}H spin–lattice relaxation times both in the laboratory and in the rotating frame were measured on PVAc sample (Tables II and III). The magnetization decays, both in the laboratory and in the rotating frame, are monoexponential (Fig. 4). The PVAc polymer shows a $T_1(H)$ value of about 3.4 s, suggesting homogeneity of the phases on this time scale. Complete homogeneity of the different regions (amorphous and crystalline) is also observed from the $T_{1\rho}(H)$ values (Table III), which defines smaller regions. The phase heterogeneities, if present, are thus smaller than 4 nm. If the dimensions of each region were large enough to avoid spin diffusion averaging the differences, a biexponential decay would have occurred [50, 51]. The $T_{1\rho}(H)$ values were also confirmed through the variable-CP-contact-time experiment (Table IV). Fig. 5 illustrates the magnetization intensity and the best fitting of Equation 2 (see exponential part) as a function of contact times for all the signals of the PVAc sample.

The $T_1(H)$ values of the PVAc–$Ca(OH)_2$ sample were found to be about 5 s. Thus we can be sure that

the alkalinity does not affect the T_1(H) values in the MDF composite but in the presence of CA or C_3A the T_1(H) values of the polymer are mainly influenced by the phase modification.

3.2. ^{13}C cross-polarization magic-angle-spinning nuclear-magnetic resonance spectra of composites containing $CaAl_2O_4$ and $Ca_3Al_2O_6$

The ^{13}C CP MAS analysis of the PVAc–CA sample (Fig. 6b) shows that complete deacetylation occurred, as shown by the absence of the peak at 22.8 ppm [6, 12–14]. From the signal resonance at 182.6 ppm of the carboxylic group, it can be deduced that acetates are formed [16]. Fig. 6a shows, for reference purposes, the ^{13}C CP MAS spectrum of aluminium acetate. The downfield carboxylic peak appears broadened and this effect could be due to the formation of calcium acetate; the methyl signal of calcium acetate (at 25.7 ppm) [16] overlaps the aluminium acetate peak at 26.7 ppm. For what concerns the methine peaks of the PVAc–CA composite, the relative intensity was different from the PVAc spectrum; the peak at 77.4 ppm partially disappeared. This effect was attributed to the loss of intramolecular hydrogen bonds of methine groups in the mm triads. Also, the peak intensity at 71.2 ppm, associated with the presence of one hydrogen bond, was reduced compared with the peak with no intramolecular hydrogen bonds (at 65.7 ppm), suggesting a marked reduction in intramolecular hydrogen bonds in the MDF composite. Probably the polymer forms intermolecular hydrogen

TABLE II Proton relaxation times in the laboratory system, T_1(H), transferring proton magnetization to ^{13}C by CP MAS NMR sequence in pure PVAc, in PVAc–C_3A and in PVAc–CA, where the values are affected by a 10% error

Assignment	Chemical shift (ppm)	T_1(H) (s)		
		PVAc	PVAc–C_3A	PVAc–CA
CH_3	22.8	3.4	ND[a]	
	26.7		0.4	0.18
CH_2	45.4	3.4		
	46.6		1.4	0.24
CH	66.0[b]	3.4	1.3	0.24
	71.3[c]	3.4	1.3	0.23
	76.6		1.0	
	77.4	3.2		
CO	169.5		0.4	0.19
	171.8	3.3		
	182.6		ND[a]	0.14

[a] ND, not determined.
[b] The exact chemical shift is 65.7 ppm.
[c] The exact chemical shift is 71.2 ppm.

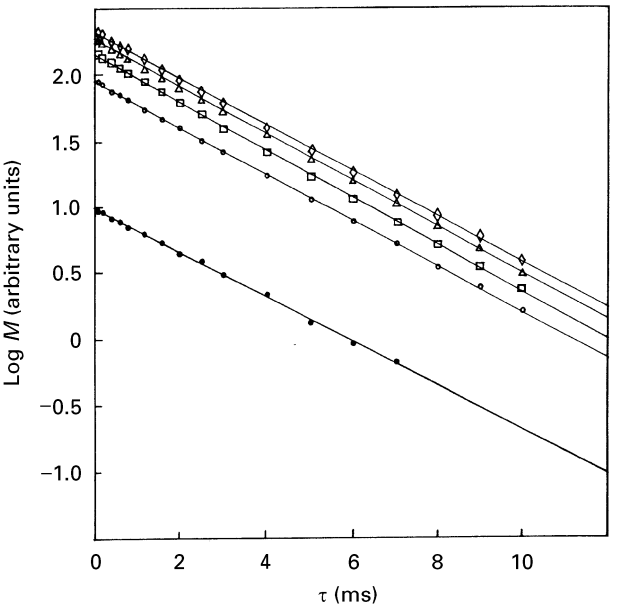

Figure 4 Variation in the logarithm of the magnetization, M, at specific times τ for measuring $T_{1\rho}$(H) values. The decays correspond to the intensity of each peak of PVAc copolymer. (●), 171.8 ppm; (○), 22.5 ppm; (□), 65.7 ppm; (△), 71.2 ppm; (◇), 45.4 ppm.

TABLE III Proton relaxation times in the rotating frame, $T_{1\rho}$(H), transferring proton magnetization to ^{13}C by CP MAS NMR sequence in pure PVAc, in PVAc–C_3A and in PVAc–CA, where the values are affected by a 10% error

Assignment	Chemical shift (ppm)	$T_{1\rho}$(H) (ms)				
		PVAc Monoexponential	PVAc–C_3A			PVAc–CA monoexponential
			Monoexponential	Biexponential	Relative percentage	
CH_3	22.8	5.5 ± 0.1	ND[a]	ND[a]		
	26.7		ND[a]	ND[a]		2.0 ± 0.2
CH_2	45.4	5.6 ± 0.1				
	46.6		4.8 ± 0.3	0.2 ± 0.1/5.3 ± 0.3	25/75	4.0 ± 0.2
CH	66.0[b]	5.3 ± 0.1	4.5 ± 0.2	0.2 ± 0.1/5.1 ± 0.2	21/79	3.8 ± 0.2
	71.3[c]	5.6 ± 0.1	4.7 ± 0.3	0.4 ± 0.2/5.5 ± 0.4	22/78	4.4 ± 0.2
	76.6		ND[a]	ND[a]		
CO	169.5		2.9 ± 0.2	0.9 ± 0.5/4.0 ± 0.8	32/68	3.9 ± 0.3
	171.8	6.0 ± 0.1				
	182.6		ND[a]	ND[a]		2.2 ± 0.4

[a] ND, not determined.
[b] The exact chemical shift is 65.7 ppm.
[c] The exact chemical shift is 71.2 ppm.

TABLE IV T_{CH} and $T_{1\rho}$(H) values measured from PVAc, where a non-linear best-fitting minimum square was applied to the intensity of each ^{13}C CP MAS NMR signal at increasing contact times and the values are affected by a 10% error

Chemical shift (ppm)	T_{CH} (ms)	$T_{1\rho}$(H) (ms)
22.8	0.54	6.3
45.4	0.17	5.4
65.7	0.12	5.1
71.2	0.15	5.4
77.4	0.19	7.0
171.8	0.55	8.5

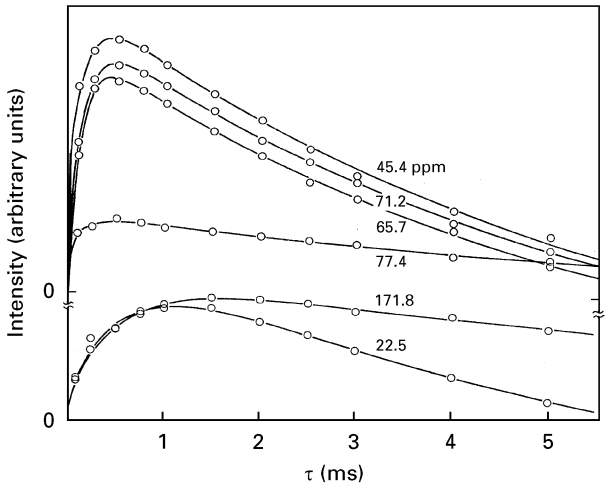

Figure 5 75.5 MHz ^{13}C CP MAS spectra at defined contact times τ of PVAc sample.

bonding with the hydrated inorganic phase and with water molecules.

The ^{13}C CP MAS spectrum of the PVAc–C_3A sample (Fig. 7b) revealed lower deacetylation (in the range of 70–80%), evidenced by the presence of the peak at 22.8 ppm, and the formation of aluminium and calcium acetate identified by the peak at 26.7 ppm for the methyl groups. As concerns the downfield region of the spectrum in Fig. 7b the signal at 182.6 ppm coincides with aluminium acetate groups (Fig. 7a). The low intensity of this peak suggests, however, that acetates must resonate also at about 170 ppm. In the same region the ester groups of the PVAc polymer are detected and the presence of carbonation products cannot be excluded [52]. As occurred in the composite containing CA, the peak intensity for methine groups is modified, but the methine peak intensity of the PVAc–C_3A sample, associated with the presence of two intramolecular hydrogen bonds (methine peaks downfield), was less reduced than that in the PVAc–CA sample. We can conclude that the polymer microstructure was more affected by the presence of the CA than the C_3A inorganic matrix.

3.3. Phase domains in aluminium-based macrodefect-free material

T_1(H) and $T_{1\rho}$(H) relaxation time measurements were performed on both composite materials. T_1(H)

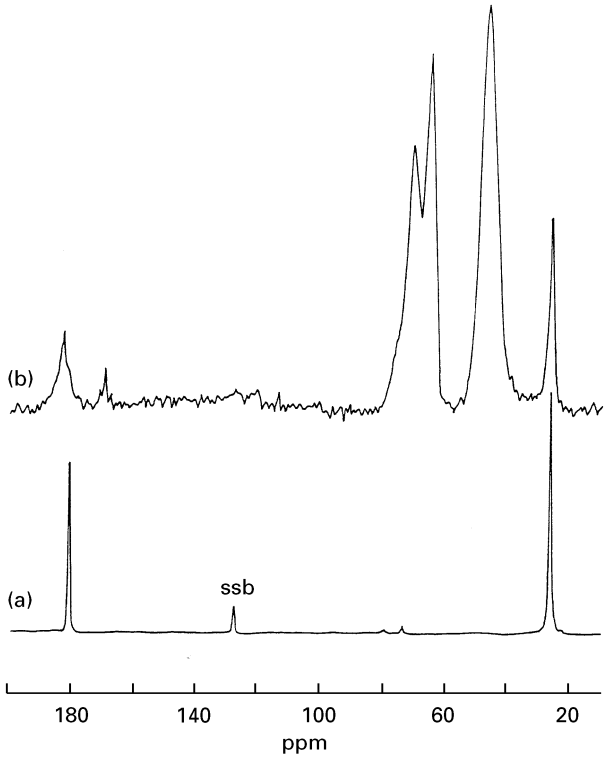

Figure 6 75.5 MHz ^{13}C CP MAS NMR spectra: (a) aluminium acetate, no resolution enhancement applied; (b) PVAc–CA pressed sample, no resolution enhancement applied. The CP mixing time was 1 ms. ssb: spinning side bands.

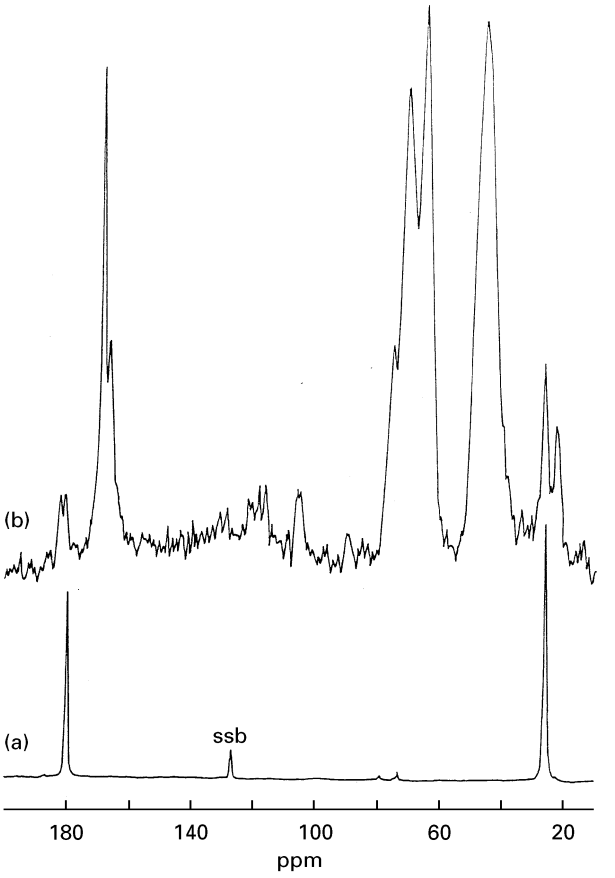

Figure 7 75.5 MHz ^{13}C CP MAS NMR spectra: (a) aluminium acetate, no resolution enhancement applied; (b) PVAc–C_3A pressed sample, line broadening refinement of 30 applied. ssb: spinning side bands.

relaxation times of the polymer in the PVAc–C_3A sample are less than 1.5 s, quite short compared with the reference polymer PVAc values (3.4 s) (Table II and Fig. 8). Although the T_1(H) values of hydrated aluminate phases were not measured, it can be supposed that proton relaxation times are shorter than those in the polymer material because of the quadrupolar nature of the aluminium nucleus. Our assumption was confirmed by looking at the T_1(H) of alumina which is as long as a few hundreds of milliseconds [53]. The T_1(H) values of 1.5 s indicate that the extension of the polymeric phases is below 80 nm. From the analysis of the peak at 26.7 ppm, acetate ions show proton relaxation times of 0.4 s. It can be concluded that the phase of the acetates is segregated with respect to the polymer matrix and probably the acetate phases are located in aluminate areas. By contrast, $T_{1\rho}$(H) measurements indicate the occurrence of two components in the polymer in the presence of C_3A (Table III). One is almost equivalent to the value of pure PVAc ($\sim$ about 5.5 ms); the other is lower than 0.5 ms. The fast component represents a minor part and is assigned to the polymeric domain, approximating the inorganic component. The polymer domains are mostly larger than 4 nm. From the T_1(H) and $T_{1\rho}$(H) values it can be deduced that the dimensions of the polymer matrix are confined within 4 and 80 nm for C_3A-based MDF composite.

The T_1(H) relaxation times of the polymer in the PVAc–CA sample were drastically reduced (Table II and Fig. 8). The values were quite short (0.2 s) compared with the reference PVAc sample, suggesting that, on the T_1(H) time scale, the dimension of the polymeric phase is not larger than the limit value of 30 nm. Each ^{13}C species showed the same values even for the acetate peaks. This indicates that the acetate phases were intimately mixed with the polymer at this time scale. The T_1(H) relaxation times of the PVAc–C_3A and PVAc–CA samples suggest a stronger influence of the inorganic phase in the sample containing CA. The $T_{1\rho}$(H) values of the PVAc–CA composite were reduced compared with those of the PVAc (Table III). The size of the polymeric region is smaller than the distances travelled by the magnetization. According to the relaxation time of 4 ms, the observation is restricted to small domains of approximately 3 nm. Compared with the measurement based on T_1(H) measurements, the system is still homogeneous on the $T_{1\rho}$(H) time scale. The acetate peak showed lower $T_{1\rho}$(H) values (2 ms) than that of the polymeric matrix (4 ms). It can be deduced that the acetate phase was segregated for dimensions of 2 nm. On comparison of T_1(H) and $T_{1\rho}$(H) values of acetate peaks in the PVAc–CA composite, the spatial arrangement of the acetate domains was confined to between 2 and 20 nm. Had the carboxylic groups been covalently bonded to the polymer, the same $T_{1\rho}$(H) would have been measured for both polymer and acetate peaks. The detection of the segregated acetate phase confirmed that the ester groups were deacetylated.

Compared with C_3A, CA shows shorter relaxation times, suggesting an efficient mixing of the phases. Moreover, a more evident loss of intramolecular hydrogen bonds was observed in the PVAc–CA composite, probably caused by the aluminium interaction. These results appear to be in agreement with previous reports proposing that chemical bonds on calcium monoaluminate surfaces exist in the form of polymer hydroxyl interactions with the aluminium atom [7–9].

It should be noted that the XRD data of both the composites gave no indication of a hydrated inorganic phase. This could be because the formation of crystalline and ordered hydrated aluminate phases was hindered.

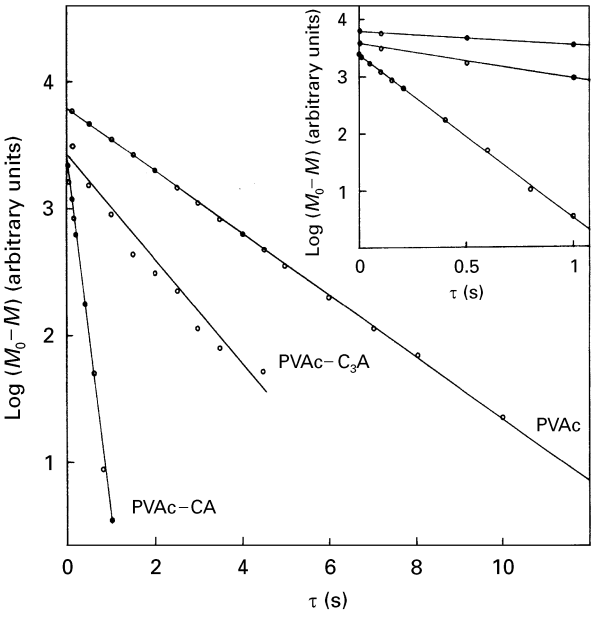

Figure 8 Logarithmic values of the intensity of magnetization, $M_0 - M$, for measuring T_1(H) values (see Section 2). M_0 is the equilibrium magnetization and M the intensity of the peak at appropriate time τ. Each point refers to the peak at 65.7 ppm at given τ for PVAc, PVAc–C_3A and PVAc–CA, respectively.

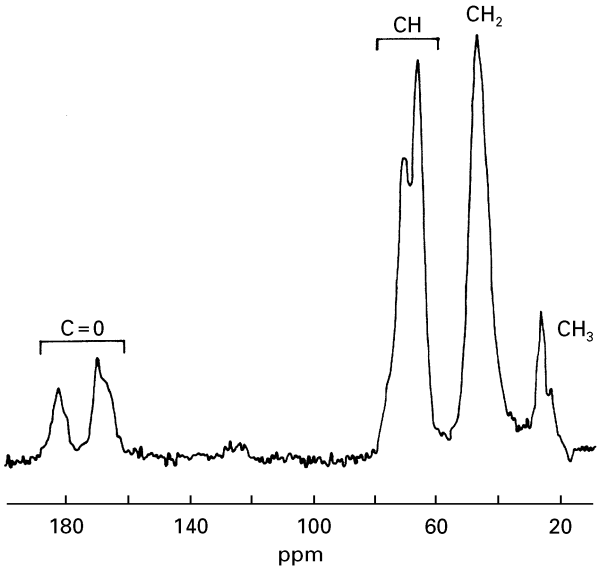

Figure 9 75.5 MHz ^{13}C CP MAS NMR spectrum of a PVAc–CA cured sample, no resolution enhancement applied. The CP mixing time was 1 ms.

3.4. Poly(vinyl alcohol)–poly(vinyl acetate)–$CaAl_2O_4$ and (poly(vinyl alcohol)–poly(vinyl acetate)–$Ca_3Al_2O_6$ cured composite

Some PVAc–CA and PVAc–C_3A materials were subjected to further curing: heating at 383 K for 24 h in an oven (atmospheric air). The ^{13}C CP MAS NMR spectrum of PVAc–C_3A did not change, suggesting that heating did not affect, at the molecular level, the deacetylation degree and the composition of chemical species in the MDF composite [54, 55]. On the contrary, the ^{13}C CP MAS NMR spectrum of the PVAc–CA composite, after curing, showed strong modification in the carboxylic region (Fig. 9). The peaks, in this region, appear broadened owing to dehydration and the signal at about 170 ppm can most probably be associated with calcium acetate and the formation of carbonate phases [54].

4. Conclusions

By observing ^{13}C NMR nuclei to measure hydrogen relaxation times in different molecular neighbourhoods we were able to determine the organic–inorganic phase interaction. This aspect was investigated by techniques recently used in the field of heterogeneous interfaces, exploiting a regime of rapid magnetization diffusion across the heterogeneous interface [16]. In this paper a further indication is given that the proton relaxation times, as observed from the carbon atoms, are sensitive to the inorganic phase, leading to the estimate of the intimacy of the phases and the quality of the interface.

Magnetization diffusion through the interfaces in PVAc–CA seems effective as regards the T_1(H) measurements. The values obtained appear to indicate that the polymer phase is greatly affected by the presence of the inorganic phase within 30 nm. The analysis of $T_{1\rho}$(H) relaxation times in the PVAc–CA composite seems to reveal that distances travelled by the magnetization in homogeneous domains are confined to a few nanometres.

In the PVAc–C_3A composite it can be affirmed that a large part of the homogeneous domains of the polymer in the composite is confined within 4 and 80 nm. Based on the $T_{1\rho}$(H) values we were able to identify a fast component possibly assigned to the organic–inorganic interphase.

With regard to localized interactions, resulting in the formation of weak bonds or specific interactions, we examined the statistical distribution of intramolecular hydrogen bonds from the chemical shift of the polymer's methine in the composite. These results led us to the conclusion that a major interaction of the polymer with the CA rather than with the C_3A inorganic matrix exists. Analysis of the methyl signals, evidenced in the ^{13}C spectrum, showed that complete deacetylation occurred in the PVAc–CA sample and only partial deacetylation in the PVAc–C_3A sample.

As regards the comparison of the interactions between partially acetylated poly(vinyl alcohol) and some of the main reactive components of cement during the hydration process including C_3S [16], a dramatic reduction in T_1 relaxation times was observed in the presently studied composites containing aluminates instead of silicates. T_1(H) relaxation times recorded through ^{13}C observations and measured on composites containing CA indicate the presence of polymeric regions of a size smaller than those occurring in the C_3A and C_3S composite obtained under the same process.

Acknowledgements

We would like to thank Dr L. Cassar of Italcementi, Bergamo, for helpful discussions. This work was partially supported by grants from Consiglio Nazionale delle Ricerche and the Italian Ministry of Education.

References

1. J. D. BIRCHALL, A. J. HOWARD and K. KENDALL, *Nature* **289** (1981) 388.
2. K. KENDALL and J. D. BIRCHALL, "Very high strength Cement-based materials", Materials Research Society Symposium Proceedings, Vol. 42 edited by J. F. Young (Materials Research Society, Pittsburgh, PA, 1985) p. 143.
3. J. D. BIRCHALL, A. J. HOWARD and K. KENDALL, Eur. Patent 0021682 (1981).
4. *Idem*., Eur. Patent 0055035 (1982).
5. K. KENDALL, A. J. HOWARD and J. D. BIRCHALL, *Phil. Trans. R. Soc. A* **310** (1983) 139.
6. O. O. POPOOLA, W. M. KRIVEN and J. F. YOUNG, *J. Amer. Ceram. Soc.* **74** (1991) 1928.
7. J. A. LEWIS and W. M. KRIVEN, *MRS Bull.* March (1993) 72.
8. O. O. POPOOLA, W. M. KRIVEN and J. F. YOUNG, *Ultramicroscopy* **37** (1991) 318.
9. O. O. POPPOLA, W. M. KRIVEN and J. F. YOUNG, in "Advanced cementitious systems: Mechanisms and properties, Materials Research Society Symposium Proceedings, Vol. 245 edited by F. P. Glasser, P. L. Pratt, T. O. Mason, J. F. Young and G. J. McCarty (Materials Research Society, Pittsburgh, PA, 1992) p. 283.
10. J. F. YOUNG, in "Specialty Cements with advanced properties", Materials Research Society Symposium Proceedings, Vol. 179 edited by B. E. Scheetz, A. G. Landers, I. Odler and H. Jennings (Materials Research Society, Pittsburgh, PA, 1991) p. 101.
11. C. S. POON and G. W. GROVES, *J. Mater. Sci.* **23** (1988) 657.
12. W. SINCLAIR and G. W. GROVES, *ibid.* **20** (1985) 2846.
13. S. A. RODGER, S. A. BROOKS, W. SINCLAIR, G. W. GROVES and D. D. DOUBLE, *ibid.* **20** (1985) 2853.
14. R. N. EDMONDS and A. J. MAJUMDAR, *ibid.* **24** (1989) 3813.
15. K. M. ATKINS, R. N. EDMONDS and A. J. MAJUMDAR, *ibid.* **26** (1991) 2372.
16. A. COMOTTI, R. SIMONUTTI and P. SOZZANI, *Chem. Mater.* **8** (1997) 2341.
17. X. CONG and R. J. KIRKPATRICK, *J. Amer. Ceram. Soc.* **76** (1993) 409.
18. J. SKIBSTED, E. HENDERSON and H. J. JAKOBSEN, *Inorg. Chem.* **32** (1993) 1013.
19. J. HJORTH, J. SKIBSTED and H. J. JAKOBSEN, *Cem. Concr. Res.* **18** (1988) 789.
20. A. RETTEL, W. GESSNER, D. MULLER and G. SCHELER, *Br. Ceram. Trans. J.* **84** (1985) 25.
21. T. LUONG, H. MAYER and H. ECKERT, *J. Amer. Ceram. Soc.* **72** (1989) 2136.
22. T. KOSMAC, G. LAHAJNAR and A. SEPE, *Cem. Concr. Res.* **23** (1993) 1.
23. M. DRABIK, L. GALIKOVA, M. KUBRANOVA and R. C. T. SLADE, *J. Mater. Chem.* **4** (1994) 265.

24. M. DRABIK, M. FRTALOVA, L. GALIKOVA and M. KRISTOFIK, *ibid.* **4** (1994) 271.
25. A. ABRAGAM, "The principles of nuclear magnetism" (Clarendon, Oxford, 1989).
26. C. A. FINCH, in "Polyvinyl alcohol-developments", edited by C. A. Finch (Wiley, Chichester, West Sussex, 1992).
27. D. W. OVENALL, *Macromolecules* **17** (1984) 1458.
28. G. VAN DER VELDEN and J. BEULEN, *ibid.* **15** (1982) 1071.
29. A. E. TONELLI, *ibid.* **18** (1985) 1086.
30. E. O. STEJSKAL and J. SCHAEFER, *J. Magn. Reson.* **18** (1975) 560.
31. D. A. TORCHIA, *ibid.* **30** (1978) 613.
32. M. MEHRING, in "High resolution NMR in solids" NMR Basic Principles and Progress Vol. 11 edited by P. Diehl, E. Fluck, H. Gunther, R. Kosfeld and J. Seelig (Springer, Berlin, 1976).
33. V. J. MCBRIERTY and K. J. PACKER, "Nuclear magnetic resonance in solid polymers" (Cambridge University Press, Cambridge, Camb, 1994).
34. J. PACKER, J. M. POPE, R. R. YEUNG and M. E. A. CUDBY„ *J. Polym. Sci., Polym. Phys. Edn* **22** (1984) 589.
35. A. M. KENWRIGHT, K. J. PACKER and B. J. SAY, *J. Magn. Reson.* **69** (1986) 426.
36. D. L. VANDERHART and A. N. GARROWAY, *J. Chem. Phys.* **71** (1979) 2773.
37. J. R. HAVENS and D. L. VANDERHART, *Macromolecules* **18** (1985) 1663.
38. L. C. DICKINSON, J-F. SHI and J. C. W. CHIEN, *ibid.* **25** (1992) 1224.
39. S. LI, L. C. DICKINSON and J. C. W. CHIEN, *J. Appl. Polym. Sci.* **43** (1991) 1111.
40. K. SCHMIDT-ROHR, J. CLAUSS, B. BLUMICH and H. W. SPIESS, *Magn. Reson. Chem.* **28** (1990) S3.
41. P. CARAVATTI, P. NEUENSCHWANDER and R. R. ERNST, *Macromolecules* **19** (1986) 1889.
42. W. GABRIELSE, H. ANGAD GAUR, F. C. FEYEN and W. S. VEEMAN, *ibid.* **27** (1994) 5811.
43. K. J. PACKER, I. J. F. POPLETT and M. J. TAYLOR, *J. Chem. Soc. Faraday Trans.* **84** (1988) 3851.
44. J.-F. MASSON and R. St JOHN MANLEY, *Macromolecules* **24** (1991) 5914.
45. P. M. HENRICHS, J. TRIBONE, D. J. MASSA and J. M. HEWITT, *ibid.* **21** (1988) 1282.
46. D. C. DOUGLASS and G. P. JONES, *J. Chem. Phys.* **45** (1966) 956.
47. T. TERAO, S. MAEDA and A. SAIKA, *Macromolecules* **16** (1983) 1535.
48. F. HORII, S. HU, T. ITO, H. ODANI, R. KITAMARU, S. MATSUZAWA and K. YAMAURA, *Polymer* **33** (1992) 2299.
49. F. IMASHIRO, S. MAEDA, K. TAKEGOSHI, T. TERAO and A. SAIKA, *J. Amer. Chem. Soc.* **109** (1987) 5213.
50. X. ZHANG, K. TAKEGOSHI and K. HIKICHI, *Polymer* **33** (1992) 712.
51. *Idem. Polym. J.* **23** (1991) 87.
52. H. W. PAPENGUTH, R. J. KIRKPATRICK, B. MONTEZ and P. A. SANDBERG, *Amer. Mineral.* **74** (1989) 1152.
53. H. D. MORRIS and P. D. ELLIS, *J. Amer. Chem. Soc.* **111** (1989) 6045.
54. H. F. W. TAYLOR, "Cement chemistry" (Academic Press, London, 1990).
55. J. F. YOUNG, *J. Amer. Ceram. Soc.* **53** (1970) 65.

Received 28 May 1996
and accepted 20 January 1997